Journal of Molecular Structure 1134 (2017) 681–686

Contents lists available at ScienceDirect

Journal of Molecular Structure

journal homepage: http://www.elsevier.com/locate/molstruc

Atomic-scale understanding of dichlorobenzene-assisted poly 3-hexylthiophene-2,5-diyl nanowire formation mechanism☆

M. Yagmurcukardes [a, *], D. Kiymaz [b], C. Zafer [b], R.T. Senger [a], H. Sahin [c]

[a] Department of Physics, Izmir Institute of Technology, 35430 Izmir, Turkey
[b] Solar Energy Institute, Ege University, Izmir, Turkey
[c] Department of Photonics, Izmir Institute of Technology, 35430 Izmir, Turkey

ARTICLE INFO

Article history:
Received 15 November 2016
Received in revised form
5 January 2017
Accepted 5 January 2017
Available online 8 January 2017

2010 MSC:
00-01
99-00

Keywords:
Density functional theory
P3HT nanowires
DCB-Assisted formation
$\pi-\pi$ interaction

ABSTRACT

Low-dimensional Poly 3-hexylthiophene-2,5-diyl (P3HT) structures that serve efficient exciton dissociation in organic solar cells, play a major role in increasing the charge collection, and hence, the efficiency of organic devices. In this study, we theoretically and experimentally investigate the Dichlorobenzene (DCB)-assisted formation of P3HT nanowires. Our experiments show that the solution of DCB molecules drive randomly oriented P3HT polymers to form well-stacked nanowires by stabilizing tail-tail and $\pi-\pi$ interactions. Here the question is how DCB molecules migrate into the P3HT layers while forming the nanowire structure. Our density functional theory-based calculations reveal that the vertical migration of the DCB molecules between P3HT layers is forbidden due to a high energy barrier that stems from strong alkyl chain-DCB interaction. In contrast to vertical diffusion, lateral diffusion of DCB molecules in between P3HT layers is much more likely. Our results show that migration of a DCB molecule occurs through the alkyl groups with a low energy barrier. Therefore, laterally diffused DCB molecules assist nucleation of top-to-top stacking of P3HT polymers and formation of well-ordered nanowires.

1. Introduction

In recent years, thiophene-based polymers became an area of interest due to their important properties such as fusibility [1] and good solubility [2]. Tunability of their structural, electronic, optical and transport properties by changing the length of side chains [3,4], temperature [5–8], molecular weight [9–15], and crystallization techniques [16,17] are some advantages for their applications. Moreover, thiophene-based semiconductor polymers are also promising materials for applications in organic electronics [18,19] due to their unique opto-electronic properties. Among these polymers, 3-hexylthiophene (P3HT) is widely studied due to its relatively higher carrier mobility [20–22]. Applications of P3HT polymers are important in light-emitting diodes [23], thin film transistors [24] and organic solar cells [25]. In addition, P3HT polymers are excellent components in photovoltaics due to their high compatibility with inorganic materials such as $TiOco_2$ [26,27], ZnO [28], and carbon nanotubes [29]. In the solar cell applications, P3HT-based solar cells have reached power conversion efficiencies of about 5% [30].

Some experimental studies on P3HT polymers clarify important unknowns about the assembly of these polymers. Prosa [31] et al. reported the P3HT self-assembling in solution by orienting the microcrystalline domains ranging between 10 and 50 nm. In addition, Prosa [32] et al. and McCullough [33] et al. claimed that P3HT in crystalline form consists of stacked planar polymer molecules. It was also reported that when a poor solvent is added on the polymer solvent, $\pi-\pi$ stacking of polymer backbones is formed by diffusive motion of poor solvent molecules [34] and van der Waals interaction between the alkyl side chains plays an important role in diffusion. Moreover, theoretical studies confirmed the lamellar structure of P3HT nanowires by atomistic simulations [35–38]. In the theoretical study by Maillard [35] et al., the energy comparison of some stacking configurations were reported by first-principles calculations based on density functional theory (DFT). Mainly two different stackings were under consideration and at zero temperature the energy difference between the two stackings of P3HT layers is quite small [35]. In another study by Melis [39] et al. it was pointed out that the $\pi-\pi$ interaction has the main contribution in

☆ Fully documented templates are available in the elsarticle package on CTAN.

* Corresponding author.
E-mail address: mehmetyagmurcukardes@iyte.edu.tr (M. Yagmurcukardes).

http://dx.doi.org/10.1016/j.molstruc.2017.01.027
0022-2860/

P3HT self-assembling. P3HT assembling at finite temperatures was also considered by using model-potential molecular dynamics (MPMD) simulations.

Very recently, we have experimentally shown [40] that the solution of DCB molecules drive randomly oriented P3HT polymers to form well-stacked nanowires by stabilizing tail-tail and $\pi-\pi$ interactions. However, how P3HT nanowires are formed at atomic level is still an open-question. In this study, by performing both experiments and *ab initio* calculations we investigate the role of DCB poor solvent in the formation of well-ordered P3HT nanowires from randomly ordered bulk P3HT phase.

The paper is organized as follows: In Sec. 2 both experimental and computational methodologies are given. The structural analysis is explained in detail experimentally and theoretically in Sec. 3. Theoretical results of the lateral and vertical migrations of a DCB molecule are given in Sec. 4.1 and Sec. 4.2, respectively. Finally, we summarize our results in Sec. 5.

2. Methods

2.1. Experimental details

The regioregular poly (3-hexylthiophene-2,5-diyl) (rr-P3HT) and the solvent of anhydrous 1, 2-DCB (99%) were purchased from Sigma-Aldrich, USA. For morphology studies, mica substrates (Grade V-4) were purchased from SPI Supplies (Catalogue number 1869-CA and Lot number 1170203).

Ambious Technology Q-Scope 250 instrument was performed in non-contact mode (tapping mode) at room temperature for topographic data. The Atomic Force Microscopy (AFM) images were obtained by using an oxide-sharpened silicon nitride cantilever with a spring constant of 48 N/m and resonance frequency of 180 kHz. The images were obtained in high spatial resolution (>7 nm tip radius). Finally, the images were analyzed by using a freeware scanning electron microscope tool of WSXM software (Nanotec Electronica SL).

Formation of P3HT nanowires was achieved as follows: 20 mg/ml (2% w/v) of bulk P3HT was dissolved in 1, 2-DCB in glass vial and stirred at 45 °C for 3 h. After dissolving the polymers completely, the solution was cooled down slowly to room temperature. Nanowire formation was performed in the solution. Firstly, temperature of the solution was decreased gradually from 27 °C to 0 °C with the rate of 4 °C/min, then the temperature was fixed at 0 °C. 10 μl P3HT solution was spin coated immediately on mica substrates at 4000 rpm for 1 min. Different spin-coated film samples were produced at certain time intervals of 15 min and 30 min, and 24 h after the preparation of the solution. The morphology of the films was examined by AFM.

2.2. Computational methodology

Simulations on migration of DCB molecule on two dimensional periodic P3HT layer were performed by using the SIESTA (Spanish Initiative for Electronic Simulations with Thousands of Atoms) [41,42] package based on DFT [43]. The code calculates the total energies and atomic forces of the simulated structure using a linear combination of atomic orbitals as the basis set. In all the calculations local density approximation (LDA) [44] was used for the exchange and correlation potential as parametrized by the Ceperley and Alder functional [45]. The interactions between electrons and core ions were simulated with separable Troullier-Martins [46] norm-conserving pseudopotentials. The convergence criteria of 0.04 eV/Å and 10^{-4} eV were considered for the forces and for the total energies in the self-consistency cycles, respectively. The electrostatic potentials were determined on a real space grid with a mesh cut off energy of 500 Ry. The geometry relaxation of the structures was performed by considering a 2×2 supercell containing eight P3HT monomers.

The minimum energy of P3HT layer was calculated for various lattice constant values and the pressure in all directions was decreased to a value smaller than 1 kBar. The Brillouin zone integration was performed by using a set of $2 \times 2 \times 1$ Monkhorst-Pack k-point sampling scheme. For the lateral migration process, all of the atoms forming the DCB molecule were fixed in lateral directions. In the case of vertical migration simulation, one of the C atoms, bound to the Cl atom was fixed along the vertical coordinate. The smearing parameter was taken as 0.01 for density of states calculations. All the calculations were performed in spin-unpolarized mode since the considered structures are non-magnetic. The binding energy per cell was calculated using the formula;

$$E_{\text{bind}} = \left[nE_{\text{monomer}} - E_{\text{periodic}} \right] \quad (1)$$

where n is the number of P3HT monomers in a unitcell while the E_{monomer} and E_{periodic} are the total energies for P3HT monomer and for its 1D or 2D periodic forms.

3. Structural analysis by atomic force microscopy

In this part, the effect of incubation time at 0 °C on P3HT nanowire formation was investigated. For this purpose P3HT solution was prepared in DCB as described in Sec. 2(A). P3HT solution was spin coated on mica substrates at certain time periods. Fig. 2 demonstrates the time variation of the surface morphology of P3HT polymers, and Table 1 summarizes the average roughness, S_a, root-mean-square roughness, S_q and the average height S_z of the films. According to the topographic measurements, the average roughness value of bulk P3HT is 1.16 nm. In the following incubation times, the average values are S_a-15min: 0.66 nm, S_a-30 min: 0.62 nm and S_a-24 h: 0.87 nm whereas the root mean square values are S_q-bulk: 1.48 nm, S_q-15min: 0.82 nm, S_q-30min: 0.78 nm and S_q-24 h: 1.09 nm. The variation of roughness values reflects the morphological change during the incubation time. Bulk P3HT (see Fig. 2(a)) at room temperature, forms dot-like P3HT islands with 120 ± 10 nm diameter and 3 ± 0.5 nm height on the surface. When the solution temperature is decreased to 0 °C, the size of dot-like islands is decreased to 60 nm resulting in a smoother morphology for both 15th minute and 30th minute samples. Besides this, at the 15th minute the first stage of formation of P3HT nanowires begins to appear like a bridge between P3HT-islands. The length of the short wires are 140 ± 20 nm and the diameters are varying between 20 nm and 40 nm. At the 30th minute, the dense network morphology is acquired by increasing the number of wires. Furthermore, length of some wires reach to 350 nm. In spite of the change in the morphology and length of the core-nanowires, there is no significant change in the diameter distribution. That result indicates that the free P3HT polymers have a tendency to join from the tip of the nanowire. At the end of 24 h, the whole surface is covered by P3HT nanowires and the islands of bulk structure is inconspicuous. The length and diameter of nanowires are about 600 nm and 40 ± 10 nm, respectively. The results point that the nucleation of nanowires begins at 0 °C in the 15th minute. The initiated core-nanowires connect the islands behaving like a bridge.

The experimental details of the formation of DCB-assisted P3HT nanowires were discussed in the previous section. Our main goal is to clarify the migration mechanism of DCB molecules into bulk P3HT structure at the atomic scale. For this purpose, here we

Table 1
Surface properties of P3HT film topographies after the incubation period.

P3HT Structure	RMS Roughness (nm)	AVG Roughness (nm)	AVG Height (nm)
Bulk-P3HT	1.48	1.16	4.83
15 min at 0 °C	0.82	0.66	2.97
30 min at 0 °C	0.78	0.62	2.21
24 h at 0 °C	1.09	0.87	2.95

perform first principles based DFT calculations on geometry relaxations for P3HT structures by considering periodic, rectangular-shaped unitcells for molecular, one-dimensional and two-dimensional structures.

The calculated binding energy per P3HT monomer, when two P3HT monomers bind from thiophene sites in vacuum, is 3.08 eV. The bonded P3HT pairs form one-dimensional conjugated backbones with a binding energy of 3.77 eV/molecule. The calculated lattice constant for this 1D structure is 7.73 Å which is in agreement with the experimental value [31] and the width of conjugated backbone is 19.93 Å that is also consistent with the reported value [47]. After forming a 1D-polymer structure, P3HT polymers prefer to form a 2D periodic monolayer by nesting from alkyl sides. The binding energy per molecule for 2D monolayer is calculated to be 377 meV per molecule. The values of 7.85 Å and 13.43 Å are calculated for the lattice parameters *a* and *b*, respectively which are in agreement with previously reported values [48]. In the next sections, we clarify how the DCB molecules migrate into the P3HT domains and form the well-ordered P3HT layers.

4. Diffusion of DCB molecule in P3HT

To clarify the role of DCB molecule through these structures, we first relax the DCB molecule in vacuum. Then for the interaction with P3HT layers the favorable interaction sites for DCB were investigated.

Geometry relaxation of DCB molecule indicates that it has a planar shape in which 4-H atoms and 2-Cl atoms are bonded to a benzene ring from each C-atom (see Fig. 1). In order to figure out the possible migration paths of DCB on a 2D P3HT layer, three main sites were considered as shown in Fig. 3. Energetically the most favorable site was calculated to be the thiophene site. This is an expected result since the interactions of benzene ring of DCB with thiophene site of 2D P3HT layer are stronger than that with the alkyl sites. Then the possible migration path of DCB over the P3HT layer is identified by considering the activation energy variations as plotted in (see Fig. 4(a)).

4.1. Lateral diffusion

The formation of P3HT nanowire is possible with the inclusion of DCB molecule into the bulk P3HT structure as mentioned before. Our previous experiments demonstrated that regularly arranged 1D-P3HT layers are organized after interacting with DCB to form P3HT nanowire. Here the question is how P3HT nanowire formation takes place with the effect of DCB. In addition, the migration mechanism of DCB through the formation of P3HT nanowire is an open question. In order to understand this interaction mechanism, first of all, three high symmetry adsorption sites on the P3HT layer were considered. During the structure optimizations on these sites, all the atoms of DCB molecule were fixed in lateral coordinates. We find that the most energetic site for DCB molecule is the thiophene site with a binding energy of 2.83 eV while the center site has a binding energy of 2.65 eV. DCB molecule has the lowest binding energy when it is placed at the tail of alkyl chain site of P3HT with a binding energy of 2.30 eV. At all three sites, DCB molecule lie fairly flat over the surface of P3HT layer.

Given a DCB molecule at the thiophene site of P3HT layer, then we investigate how it would negotiate its way across the layer. The lateral migration mechanism of DCB in a rectangular mesh whose

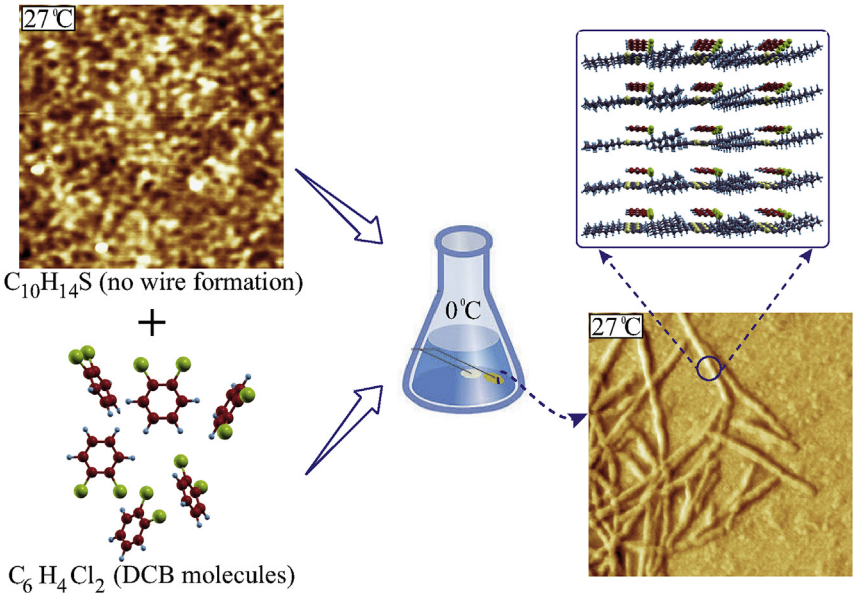

Fig. 1. Schematic illustration of P3HT nanowire formation. The top-left AFM-image shows the bulk form of P3HT in which there are randomly stacked P3HT layers while bottom-right AFM-image shows the formed nanowire.

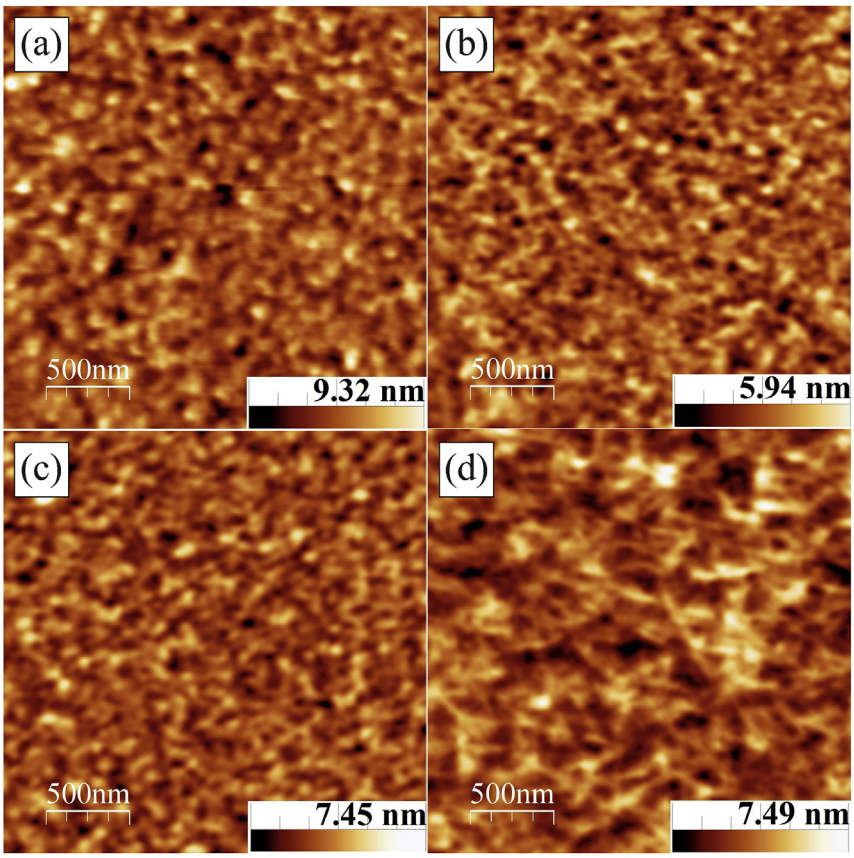

Fig. 2. Topographic AFM images of (a) bulk P3HT at room temperature, and the films grown from the solution at 0 °C for (b) 15 min, (c) 30 min and (d) for 24 h.

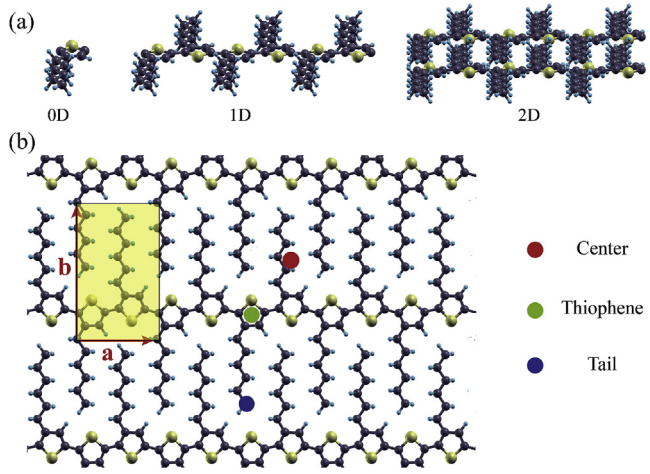

Fig. 3. Tilted view of (a) Monomer (0D), one dimensional polymer (1D) and two dimensional single layer (2D) forms of P3HT, (b) highly favored adsorption sites of DCB molecule on a P3HT layer where *a* and *b* are lattice vectors along lateral directions.

corners are at thiophene sites (see Fig. 4(a)) was investigated. The distance from a thiophene site to another across *b* direction is 13.43 Å while this distance is 7.85 Å along the *a* direction. The variations of the E_a were calculated in this rectangular mesh and are given in Fig. 4(a). For the migration of DCB through the mesh, maximum E_a value is about 0.64 eV. There is a smooth increase in the total energy of the system along the migration path from alkyl chain site to thiophene site. Although the P3HT layer is symmetric and periodic, the change in E_a is not symmetric. This anti-symmetric E_a change occurs because the Cl-site of DCB molecule is not rotating while it migrates. DCB molecules fill the thiophene sites first, the lowest energy site, then the alkyl chain site is an option for DCB to migrate from thiophene site but an energy of 0.64 eV is required. The blue regions in Fig. 4(a) indicate the possible migration path of DCB on P3HT layer with minimum E_a. Although there exist high E_a regions shown by red contours in Fig. 4(a) when compared to the thermal energy at room temperature which is 26 meV, it is possible for DCB to migrate to the alkyl chain site at higher temperatures. In addition, it should be noted that this E_a value is usually overestimated by LDA, so it is expected to be lower in reality.

Our calculations indicate that the maximum E_a of 0.2 eV is required for migration of DCB from one thiophene site to another one along the *a* direction through the blue regions shown in Fig. 4(a). When compared to that of thiophene-thiophene migration path along *b*, E_a has a much smaller value for the migration of DCB. Thus as a realistic scenario, we conclude for the lateral migration that DCB molecules as follows. First it prefers to be adsorbed on thiophene site of P3HT layer. After adsorption on this site, migration of the molecule is possible to the center site. DCB molecule might be then adsorbed on alkyl chain site due to a relatively high E_a value for the migration along the alkyl-thiophene sites path. For two different lateral migration paths, although E_a values are high compared to room temperature value of thermal energy, the migration of DCB is still possible through these paths when compared to the vertical migration through the layer since it is ensured experimentally that the formation of P3HT nanowire with the help of DCB molecule is possible.

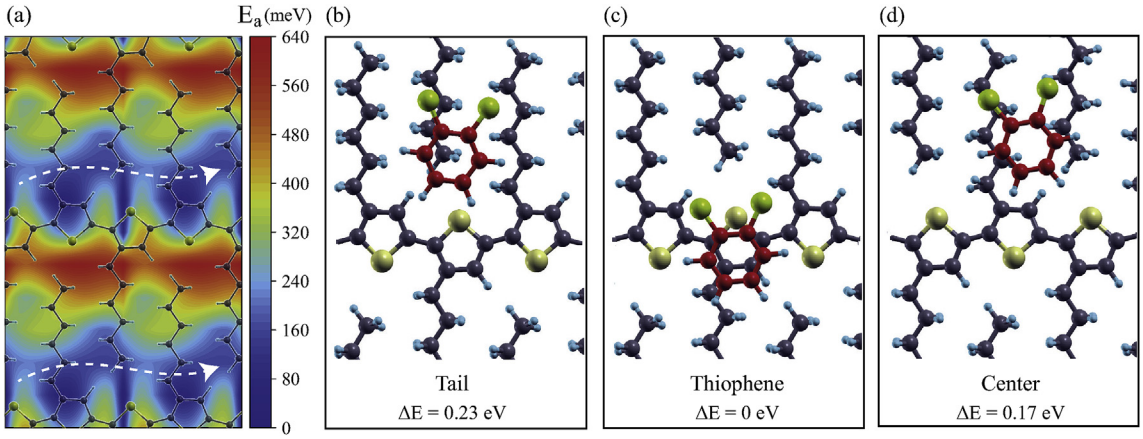

Fig. 4. (a) Contour plot of the activation energy, E_a, for lateral migration and top view of DCB on (b) Alkyl chain, (c) Thiophene and (d) Center sites, respectively. White dashed arrows in part (a) demonstrate the possible migration path for DCB molecule.

4.2. Vertical diffusion

As mentioned before, the lateral migration of DCB is possible through the P3HT layer between different adsorption sites. We also study the possible vertical migration of the molecule from one layer to another. For this purpose, one C atom of the DCB molecule was fixed along the vertical coordinate and it was set free to relax along the lateral directions. Also all the atoms in the two thiophene sites near the DCB molecule were fixed for the vertical coordinate. Our geometry optimizations indicate that when DCB molecule is adsorbed on the center site, it is on top of the junction of two tails of alkyl chains as seen in Fig. 4(d). Thus the vertical migration of DCB from one layer to another may be possible through the center site. Initially DCB molecule is parallel to the P3HT layer at center site with a vertical distance of 1.9 Å. The vertical distance between the molecule and layer is decreased by 1.0 Å in each step and the system is relaxed with the calculation of total energy. The distance Δ z is defined as the distance between the fixed C atom and the fixed thiophene site as seen in Fig. 5(b)-(e). When DCB molecule starts to enter into the layer, the tails interacting with the molecule move in lateral directions to open a hole for the molecule. And the molecule rotates vertically downward and dip into the layer from the opened-tails of alkyl chain. Up to this configuration the activation energy (E_a) is about 0.6 eV which seems to be low for a possible vertical migration. However, after that point as the DCB migrate to another layer vertically, tails interacting with DCB start to move vertically downward along the direction of motion of the molecule. This is because of the strong interaction of DCB with the tails which causes the E_a to get larger and larger up to a value of 2.5 eV which precludes the vertical migration of DCB. Although this value is overestimated by LDA, the vertical migration of DCB seems to be impossible from one layer to another. As we mentioned in the above part of the study, it is ensured that the DCB molecule migrate through P3HT layer to form the P3HT nanowire. Our results indicate that DCB can not migrate vertically through P3HT layers because of its high E_a value as compared to E_a a for lateral migration path.

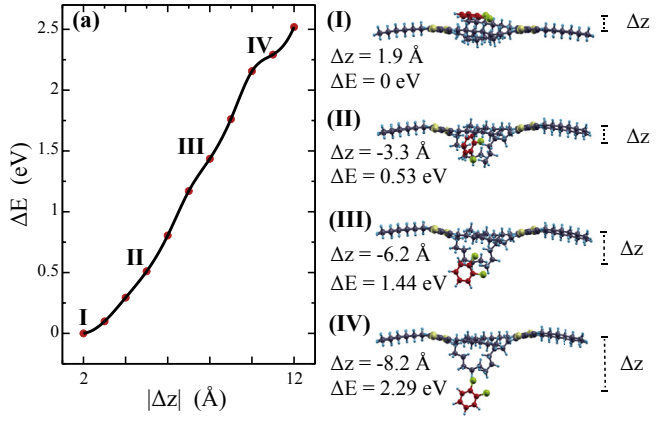

Fig. 5. Change of total energy of system under vertical migration of DCB through P3HT layer and position of DCB at different steps.

5. Conclusion

Our study points out that the nanowire formation is possible when P3HT interacts with both of DCB molecule. Thus, here our goal is to explain in details the interaction mechanism of DCB with P3HT layers while it migrates into the layers. Our study revealed that when DCB molecule is added to bulk P3HT, it organizes the 1D-P3HT polymers to form 2D layers by strong tail-tail interaction. For the migration of DCB through the P3HT layers we found that only lateral migration is possible because of the relatively small E_a barrier when compared to that of the vertical migration. The highest binding energy between DCB and P3HT layer exists for thiophene site of the layer. Thus lateral migration is possible from thiophene site to alkyl site and center sites, respectively. It is also pointed out that the vertical migration of the molecule is impossible due to the high E_a barrier. We conclude that when DCB molecules are added to bulk P3HT they enter into the layers from sides of P3HT layers. Our combined study of theory and experiment reveals that randomly oriented P3HT monomers may form stable well-stacked nanowires upon the lateral migration of solvents such as DCB.

Acknowledgements

Computational resources were provided by TUBITAK ULAKBIM, High Performance and Grid Computing Center (TR-Grid e-Infrastructure). H.S. acknowledges financial support from the Scientific and Technological Research Council of Turkey (TUBITAK) under the project number 116C073. H.S. acknowledges support from Bilim Akademisi - The Science Academy, Turkey under the BAGEP program.

References

[1] K. Yoshino, D.H. Park, B.K. Park, M. Onoda, R.-I. Sugimoto, Electrical and optical properties of poly (3-alkylthiophene) in liquid state, Solid state Commun. 67 (12) (1988) 1119–1121.

[2] M. Winokur, D. Spiegel, Y. Kim, S. Hotta, A. Heeger, Structural and absorption studies of the thermochromic transition in poly (3-hexylthiophene), Synth. Met. 28 (1) (1989) 419–426.

[3] R.D. McCullough, S.P. Williams, Toward tuning electrical and optical properties in conjugated polymers using side-chains: highly conductive head-to-tail, heteroatom functionalized polythiophenes, J. Am. Chem. Soc. 115 (24) (1993) 11608–11609.

[4] Y.D. Park, D.H. Kim, Y. Jang, J.H. Cho, M. Hwang, H.S. Lee, J.A. Lim, K. Cho, Effect of side chain length on molecular ordering and field-effect mobility in poly (3-alkylthiophene) transistors, Org. Electron. 7 (6) (2006) 514–520.

[5] J. Corish, D. Feeley, D. Morton-Blake, F. Beniere, M. Marchetti, Atomistic investigation of thermochromism in a poly (3-alkylthiophene), J. Phys. Chem. B 101 (48) (1997) 10075–10085.

[6] M. Leclerc, C. Roux, J.-Y. Bergeron, Structural effects on the thermochromic properties of polythiophene derivatives, Synth. Met. 55 (1) (1993) 287–292.

[7] K. Yoshino, S. Nakajima, H.B. Gu, R.-I. Sugimoto, Absorption and emission spectral changes in a poly (3-alkylthiophene) solution with solvent and temperature, Jpn. J. Appl. Phys. 26 (12A) (1987) L2046.

[8] Z. Wu, A. Petzold, T. Henze, T. Thurn-Albrecht, R.H. Lohwasser, M. Sommer, M. Thelakkat, Temperature and molecular weight dependent hierarchical equilibrium structures in semiconducting poly (3-hexylthiophene), Macromolecules 43 (10) (2010) 4646–4653.

[9] R.J. Kline, M.D. McGehee, E.N. Kadnikova, J. Liu, J.M. Fréchet, M.F. Toney, Dependence of regioregular poly (3-hexylthiophene) film morphology and field-effect mobility on molecular weight, Macromolecules 38 (8) (2005) 3312–3319.

[10] R.J. Kline, M.D. McGehee, M.F. Toney, Highly oriented crystals at the buried interface in polythiophene thin-film transistors, Nat. Mater. 5 (3) (2006) 222–228.

[11] M. Brinkmann, P. Rannou, Effect of molecular weight on the structure and morphology of oriented thin films of regioregular poly (3-hexylthiophene) grown by directional epitaxial solidification, Adv. Funct. Mater. 17 (1) (2007) 101–108.

[12] M. Brinkmann, P. Rannou, Molecular weight dependence of chain packing and semicrystalline structure in oriented films of regioregular poly (3-hexylthiophene) revealed by high-resolution transmission electron microscopy, Macromolecules 42 (4) (2009) 1125–1130.

[13] A. Zen, M. Saphiannikova, D. Neher, J. Grenzer, S. Grigorian, U. Pietsch, U. Asawapirom, S. Janietz, U. Scherf, I. Lieberwirth, et al., Effect of molecular weight on the structure and crystallinity of poly (3-hexylthiophene), Macromolecules 39 (6) (2006) 2162–2171.

[14] S. Joshi, S. Grigorian, U. Pietsch, X-ray structural and crystallinity studies of low and high molecular weight poly (3-hexylthiophene), Phys. status solidi (a) 205 (3) (2008) 488–496.

[15] S. Joshi, S. Grigorian, U. Pietsch, P. Pingel, A. Zen, D. Neher, U. Scherf, Thickness dependence of the crystalline structure and hole mobility in thin films of low molecular weight poly (3-hexylthiophene), Macromolecules 41 (18) (2008) 6800–6808.

[16] N. Kayunkid, S. Uttiya, M. Brinkmann, Structural model of regioregular poly (3-hexylthiophene) obtained by electron diffraction analysis, Macromolecules 43 (11) (2010) 4961–4967.

[17] L.H. Jimison, M.F. Toney, I. McCulloch, M. Heeney, A. Salleo, Charge-transport anisotropy due to grain boundaries in directionally crystallized thin films of regioregular poly (3-hexylthiophene), Adv. Mater. 21 (16) (2009) 1568–1572.

[18] A.J. Heeger, Semiconducting and metallic polymers: the fourth generation of polymeric materials, J. Phys. Chem. B 105 (36) (2001) 8475–8491.

[19] M.L. Chabinyc, A. Salleo, Materials requirements and fabrication of active matrix arrays of organic thin-film transistors for displays, Chem. Mater. 16 (23) (2004) 4509–4521.

[20] Z. Bao, A. Dodabalapur, A.J. Lovinger, Soluble and processable regioregular poly (3-hexylthiophene) for thin film field-effect transistor applications with high mobility, Appl. Phys. Lett. 69 (26) (1996) 4108–4110.

[21] H. Sirringhaus, N. Tessler, R.H. Friend, Integrated optoelectronic devices based on conjugated polymers, Science 280 (5370) (1998) 1741–1744.

[22] M. Raja, G. Lloyd, N. Sedghi, W. Eccleston, R. Di Lucrezia, S. Higgins, Conduction processes in conjugated, highly regio-regular, high molecular mass, poly (3-hexylthiophene) thin-film transistors, J. Appl. Phys. 92 (3) (2002) 1441–1445.

[23] M. Valadares, I. Silvestre, H. Calado, B. Neves, P. Guimarães, L. Cury, Behp-ppv and p3ht blends for light emitting devices, Mater. Sci. Eng. C 29 (2) (2009) 571–574.

[24] B. Gburek, V. Wagner, Influence of the semiconductor thickness on the charge carrier mobility in p3ht organic field-effect transistors in top-gate architecture on flexible substrates, Org. Electron. 11 (5) (2010) 814–819.

[25] H. Hoppea, N.S. Sariciftci, Organic solar cells: an overview, J. Mater. Res. 19 (7) (2004) 1925.

[26] K.M. Coakley, M.D. McGehee, Photovoltaic cells made from conjugated polymers infiltrated into mesoporous titania, Appl. Phys. Lett. 83 (16) (2003) 3380–3382.

[27] P. van Hal, M. Christiaans, M. Wienk, J. Kroon, R. Janssen, Ajj Phys. Chem. B 102 (1999) 4352–4359.

[28] S. Günes, N.S. Sariciftci, Hybrid solar cells, Inorg. Chim. Acta 361 (3) (2008) 581–588.

[29] M. Giulianini, E.R. Waclawik, J.M. Bell, M. Scarselli, P. Castrucci, M. De Crescenzi, N. Motta, Poly (3-hexyl-thiophene) coil-wrapped single wall carbon nanotube investigated by scanning tunneling spectroscopy, Appl. Phys. Lett. 95 (14) (2009) 143116.

[30] W. Ma, C. Yang, X. Gong, K. Lee, A.J. Heeger, Thermally stable, efficient polymer solar cells with nanoscale control of the interpenetrating network morphology, Adv. Funct. Mater. 15 (10) (2005) 1617–1622.

[31] T. Prosa, M. Winokur, J. Moulton, P. Smith, A. Heeger, X-ray structural studies of poly (3-alkylthiophenes): an example of an inverse comb, Macromolecules 25 (17) (1992) 4364–4372.

[32] T. Prosa, M. Winokur, R. McCullough, Evidence of a novel side chain structure in regioregular poly (3-alkylthiophenes), Macromolecules 29 (10) (1996) 3654–3656.

[33] R.D. McCullough, S. Tristram-Nagle, S.P. Williams, R.D. Lowe, M. Jayaraman, Self-orienting head-to-tail poly (3-alkylthiophenes): new insights on structure-property relationships in conducting polymers, J. Am. Chem. Soc. 115 (11) (1993) 4910–4911.

[34] N. Kiriy, E. Jähne, H.-J. Adler, M. Schneider, A. Kiriy, G. Gorodyska, S. Minko, D. Jehnichen, P. Simon, A.A. Fokin, et al., One-dimensional aggregation of regioregular polyalkylthiophenes, Nano Lett. 3 (6) (2003) 707–712.

[35] A. Maillard, A. Rochefort, Structural and electronic properties of poly (3-hexylthiophene) π-stacked crystals, Phys. Rev. B 79 (11) (2009) 115207.

[36] J.E. Northrup, Atomic and electronic structure of polymer organic semiconductors: P3ht, pqt, and pbttt, Phys. Rev. B 76 (24) (2007) 245202.

[37] E. Johansson, S. Larsson, Electronic structure and mechanism for conductivity in thiophene oligomers and regioregular polymer, Synth. Met. 144 (2) (2004) 183–191.

[38] Y.-K. Lan, C.-I. Huang, A theoretical study of the charge transfer behavior of the highly regioregular poly-3-hexylthiophene in the ordered state, J. Phys. Chem. B 112 (47) (2008) 14857–14862.

[39] C. Melis, L. Colombo, A. Mattoni, Self-assembling of poly (3-hexylthiophene), J. Phys. Chem. C 115 (2) (2010) 576–581.

[40] D. Kiymaz, M. Yagmurcukardes, A. Tomak, H. Sahin, R. Senger, F. Peeters, H. Zareie, C. Zafer, Controlled growth mechanism of poly (3-hexylthiophene) nanowires, Nanotechnology 27 (45) (2016) 455604.

[41] P. Ordejón, E. Artacho, J.M. Soler, Self-consistent order-n density-functional calculations for very large systems, Phys. Rev. B 53 (16) (1996) R10441.

[42] J.M. Soler, E. Artacho, J.D. Gale, A. García, J. Junquera, P. Ordejón, D. Sánchez-Portal, The siesta method for ab initio order-n materials simulation, J. Phys. Condens. Matter 14 (11) (2002) 2745.

[43] W. Kohn, L.J. Sham, Self-consistent equations including exchange and correlation effects, Phys. Rev. 140 (4A) (1965) A1133.

[44] J.P. Perdew, A. Zunger, Self-interaction correction to density-functional approximations for many-electron systems, Phys. Rev. B 23 (10) (1981) 5048.

[45] D.M. Ceperley, B. Alder, Ground state of the electron gas by a stochastic method, Phys. Rev. Lett. 45 (7) (1980) 566.

[46] N. Troullier, J.L. Martins, Efficient pseudopotentials for plane-wave calculations, Phys. Rev. B 43 (3) (1991) 1993.

[47] S.A. Chen, J.M. Ni, Structure/properties of conjugated conductive polymers. 1. neutral poly (3-alkythiophene) s, Macromolecules 25 (23) (1992) 6081–6089.

[48] D. Kim, J.T. Han, Y. Park, Y. Jang, J. Cho, M. Hwang, K. Cho, Single-crystal polythiophene microwires grown by self-assembly, Adv. Mater. 18 (6) (2006) 719–723.